Pergamon

Tetrahedron 57 (2001) 5715–5729

TETRAHEDRON

Aromaticity indices revisited: refinement and application to certain five-membered ring heterocycles

Serghey I. Kotelevskii[a] and Oleg V. Prezhdo[b,*]

[a]*Research Institute for Chemistry, Kharkiv National University, Svobody Square 4, 61077 Kharkiv, Ukraine*
[b]*Department of Chemistry, University of Washington, Seattle, WA 98195-1700, USA*

Received 14 November 2000; accepted 2 May 2001

Abstract—Three simple improvements are introduced into the conventional Bird and Pozharskii systems of the structural aromaticity indices (AIs) to eliminate discrepancies between them. The Gordy bond length/bond order relationship is re-calibrated from the experimental bond lengths. Cyclopentadiene molecule with the geometry from MW has been chosen as a unified reference structure with no aromaticity. The scheme of Pozharskii is augmented with normalization by the mean bond order. Using the refined AIs, several regularities in the aromaticity of the azoles as a function of both chemical structure and environment have been specified.

1. Introduction

The problem of an efficient and accurate semi-quantitative characterization of aromaticity, and heteroaromaticity as a special case, remains of current interest as a number of reviews suggest.[1–7] There has been a great progress in the field during the last decade, and a much deeper insight into the problem of aromaticity is possible now. After the pioneer work of Jug and Koster[8] on the one hand, and the principal component analysis studies carried out by several workers[9–11] on the other, there became evident the multi-dimensional nature of the aromatic behavior. The set of properties usually being referred to as 'aromaticity' is definable via at least two groups of criteria, namely, 'classical' and 'magnetic' ones. A comprehensive survey of the aromaticity criteria can be found in the literature, see e.g. Refs. 1, 2, 12.

Recent evidence[13–15] indicates that classical and magnetic aromaticity criteria, in fact, may be strongly correlated. As follows from the series of papers on HOMA by Krygowski and co-workers,[16–20] it is the geometric features that integrate the bulk of information on the classical aromatic character of the ring system. These findings revive the interest to the simple classical indices, including the structural aromaticity indices (SAI) first proposed by Fringuelli et al.,[21] Pozharskii,[22] and Bird.[23,24]

Along with many direct experimental techniques, SAI became an increasingly popular tool in the studies of aromatic molecular structures. SAI are easy to use. They allow evaluation and comparison of relative aromaticities of both entire molecules and any of the molecular submoieties, thus providing an advantage over the much more sophisticated corresponding experimental techniques.

At present, two independent systems of SAI are widely used. The first one was proposed by Pozharskii[22] and conceptually goes back to the work of Fringuelli et al.[21] The second one is due to Bird.[23] Both systems define the aromaticity criterion via the degree of uniformity of the peripheral bond orders (BO).

In principle, the bond orders required in the definition of SAI can be obtained from direct quantum-chemical calculations.[25] A more general approach, however, is based on molecular geometries that are available from many experimental and theoretical studies. The BOs N are evaluated from the experimental or calculated bond lengths R according to the Gordy relationship[26]

$$N = a/R^2 - b \tag{1}$$

employing a unified set of the a and b values. The distinction between the aromaticity systems of Pozharskii[22] and Bird[23] comes in the averaging of the BO fluctuations and the definition of the bond non-uniformity measure. The Pozharskii index is calculated using the average of the absolute BO differences

$$V = \overline{\Delta N} = \frac{\sum \Delta N}{n} \tag{2}$$

The SAI of Bird uses the root-mean-square deviation of

Keywords: heteroaromaticity; heterocycles; aromaticity indices.
* Corresponding author. Fax: +1-206-522-1602;
e-mail: prezhdo@u.washington.edu

0040–4020/01/$ - see front matter
PII: S0040-4020(01)00485-9

individual BOs from their arithmetic mean

$$V = \frac{100}{\bar{N}}\sqrt{\frac{\sum(N-\bar{N})^2}{n}} \quad (3)$$

In both cases, the aromaticity index (AI) of a sample structure is calculated in per cent relative to the aromaticity of benzene using the relation

$$\mathrm{AI} = 100(1 - V_s/V_R) \quad (4)$$

where V_S and V_R are the measures of the BO non-uniformity for the sample and reference structures, respectively. The reference structure is assumed fully localized with zero aromaticity.

Although both systems are constructed using the same sets of experimental data, notable discrepancies[7] between the two systems exist in both absolute and relative aromaticities. For example, the aromaticities of furan relative to benzene are calculated to be 12% by the Pozharskii system and 43% using the system of Bird. Triazoles appear to be more aromatic than the tetrazolium ion according to the scheme of Pozharskii, whereas the Bird system predicts the opposite order. When the systems of AI are applied to study the dependence of aromaticity on molecular structure or environment,[12] excessive attention is often drawn to the distinct behavior of the two systems. It is due to the observed discrepancies that some experts[7] conclude that neither of the SAI systems is reliable and that the use of either system is limited only within series of closely related molecules.

The present paper analyses the sources of the discrepancies between the two AI systems. The proposed solution significantly improves mutual consistency of the two systems. With modified AIs as a tool, structural and environmental regularities in aromaticities are explored in the azole series.

2. Theory

Preliminary analysis of the AI systems of Bird and Pozharskii suggests three possible sources of discrepancy between the systems:

(i) use of inconsistent *a* and *b* values;
(ii) difference in the reference structures in two cases;
(iii) lack of the average BO correction within the Pozharskii scheme.

These three sources of discrepancy can be interrelated. For instance, inconsistent *a* and *b* values can enhance the differences between the arithmetic mean of BOs of the Pozharskii scheme and the root-mean-square mean of the Bird treatment.

In order to improve consistency of the *a* and *b* values, we have revised the original data of Gordy[26] on the bond order/bond length relationship. The relationship is intended for use primarily with experimental data. Therefore, it is appropriate to recalibrate the *a* and *b* values based solely on the experimentally observed values of bond lengths. The lengths of most ordinary and multiple bonds are currently available with great accuracy from direct experimental techniques. As a result, approximate estimates for bond lengths, such as those based on the Shoemaker–Stevenson relationship

$$R_{AB} = r_A + r_B - |\chi_A - \chi_B| \quad (5)$$

used by Gordy, can be replaced by direct experimental data. The use of experimental data for bond lengths suggest that the calibration of the *a* and *b* parameters can be obtained from empirical counterparts of bond orders, i.e. bond multiplicities, rather than based on BOs from various weakly related sets of quantum chemical calculations as was done by Gordy. Multiplicities are known to be highly characteristic for the common types of chemical bond (e.g. C–C, C–O, etc.) in organic molecules provided that the state of hybridization is fixed for both atoms in the bond.

In this work, the Gordy relationship (1) is re-calibrated using the reliable experimental data on the lengths of the formally single, double and, whenever possible, triple bonds taken from Refs. 27–31. The bond lengths used for calibration are derived mostly from the microwave spectroscopy data. Representative values obtained from crystallographic structures are also included. Care is taken to avoid steric hindrance and other influences that might disturb the pure hybridization states of the atoms. As a result, several bond length/bond multiplicity pairs are selected for each of the common bond types. These selected values are fitted to the Gordy linear relationship with the ORIGIN 5.0 software[32] to yield the refined values of *a* and *b*. The refined *a* and *b* values together with the accuracy limits are presented in Table 1 along with the earlier data of Gordy.

As can be seen from Table 1, the greatest deviation from the previous values is observed for the N–O and N–N bonds, the type of bond poorly characterized in the earlier works. The difference comes maily from erroneous lengths of the single bonds in hydrazines and hydroxylamines. According to our data, the contribution of these bonds to the overall molecular aromaticity is rather different from that believed previously. While it is not surprising to obtain new parameters for the N–O and N–N bonds, the differences between the refined and original Gordy parameters have

Table 1. The *a* and *b* coefficients in the Gordy relationship (1) refined according to the experimental data on bond lengths. For comparison, the earlier data of Gordy[25] are given in parentheses

Bond type	C–C	C–N	C–O	C–S[a]	N–O[a]	N–N
a	7.366±0.070 (6.80)	6.941±0.146 (6.48)	5.315±0.094 (5.75)	11.250 (11.9)	4.634 (4.98)	6.132±0.069 (5.28)
b	2.115±0.035 (1.71)	2.205±0.075 (2.00)	1.616±0.054 (1.85)	2.400 (2.59)	1.165 (1.41)	1.916±0.040 (1.41)

The refined values include accuracy estimates.
[a] The values for these bonds are given without accuracy estimates since these were derived from average bond lengths taken from the literature.

been less expected for the C–C bond. The observed difference is mainly due to the overestimation of the ordinary C–C bond length that was taken to be 1.55 Å by Gordy. The average of the currently accepted C–C bond lengths[27–31] is 1.538 Å. This value is used in the present study. An essential difference in both *a* and *b* parameters for the C–O bond arises from the overestimation of the double C=O bond length taken by Gordy as 1.22 Å compared to the present averaged value of 1.214 Å.

The *a* and *b* values derived from the experimentally available bond lengths for the integer bond multiplicities are applied to intermediate lengths to obtain the corresponding intermediate BOs. The problems associated with this procedure are discussed in the paper of Box[33] who found that the chemical bonds tend to conserve themselves in the integer units, while the corresponding BO varies within the range of ±0.5. The equivalence of BO to bond multiplicity is therefore broken at the intermediate bond lengths and BOs. Similarly, Witanowski and Biedrzycka[34] in their NMR study were unable to distinguish between the bonds of the different lengths from the NMR spin–spin couplings, while a clear distinction was found between the C–C bonds being formally double or single. In this study, we apply the term bond localization to the bond lengths and bond orders, in contrast to the bond multiplicities of Box.[33]

The choice of the reference structure with zero aromaticity constitutes the second and, perhaps, the most essential source of the discrepancy between the two systems of AIs. The system of Bird takes reference in the localized Kekulé structure with alternating single and double bonds. For the five-membered ring heterocycles this gives the variation in the bond orders of $V = 35$.[23] Pozharskii, on the other hand, uses the cyclopentadiene molecule (CPD) as the reference of zero aromaticity. The source of the molecular geometry of CPD is not clear from the context.[22] To eliminate this uncertainty, we use the currently available geometry of CPD derived by the microwave spectroscopy[29] with the bond lengths of R_{CH_2}–CH=1.509 Å, $R_{CH=CH}$=1.342 Å, and R_{CH-CH}=1.469 Å. The CPD reference structure corresponds to the cyclic conjugated diene rather than to the ideal Kekulé structure. It should be noted that the bond lengths accepted for CPD are very close to those in open-chain polyenes that are conventionally used as reference in REPE calculations. For example, compare the above data with the bond lengths of butadiene $R_{C=C}$=1.345 Å, R_{C-C}= 1.465 Å obtained from MW data.

The CPD molecule significantly changes its geometry in crystal.[28,35] For instance, among other changes, the perfect C_{2V} molecular symmetry is broken in the crystal phase. An ambiguity arises whether the MW or the X-ray structure should be used as the proper reference when compared to X-ray data for other molecules. The C_{2V} MW structure appears to be a more preferable reference in most cases provided that the changes in the AIs due to the environment in the crystal phase are treated in terms of bond localization rather than in terms of aromaticity. A more detailed discussion of this issue will be presented below.

The third source of the mismatch between the AIs calculated according to Bird and Pozharskii comes from the fact that the arithmetic mean BO changes from one molecular cycle to another. This change is properly treated in the Bird scheme, where the root-mean-square of the BO deviation is normalized by the arithmetic mean BO, $\bar{N}$, see Eq. (3). No such correction is introduced in the original treatment of Pozharskii. In this study, we modify the Pozharskii scheme by dividing the sum of the BO deviations by $\bar{N}$ in both the sample and the reference structures.

$$V\ (\%) = 100\frac{\overline{\Delta N}}{\bar{N}} \tag{6}$$

Due to normalization by $\bar{N}$, the possible dependence of aromaticity upon the mean molecular BO is excluded. Within the harmonic oscillator model of aromaticity (HOMA) by Krygowski and Cyranski,[5,20,36] the overall aromaticity in the hydrocarbon and heterocyclic series tends to decrease with bond elongation above the optimal bond length. In our scheme, the BO variation *V* becomes greater if not divided by the larger value of $\bar{N}$. Qualitatively, this provides for AIs the same decrease with the bond elongation as that obserwed for HOMA by Krygowski and Cyranski. However, the trend is hardly so simple that it may be properly introduced by discarding the normalization. Whether or not to normalize the BO variation by $\bar{N}$ is therefore a matter of discussion. However, the choice should be consistent in both schemes.

Once the above changes in the aromaticity schemes are made, the discrepancy between the two AI scales is expected to decrease. In order to test the expected improvement, we have recalculated the AIs for a number of oxa and aza five-membered heterocycles. The structures of the five-membered heterocycles under study are listed in Figure 1 below. Both electrically neutral and protonated and anionic species are included into consideration. The assumption is made that the unified set of *a* and *b* values is applicable to all these systems regardless of the charge.

The AIs are calculated with the refined *a* and *b* values, that are listed in Table 1, and relative to the reference cyclopentadiene structure derived from the MW spectroscopy. Two sets of AIs are obtained in the Pozharskii scheme. The first set is calculated by the originally proposed formula (2). The second set is calculated with the BO normalization, Eq. (6). For every crystal structure derived from the X-ray data, neutron diffraction data, etc., additional AI values are calculated relative to the X-ray CPD reference structure.

The following are the V_R values of the reference structures obtained in this study and given in percent: V_R=26.377 for CPD(MW),[29] 29.791 for CPD(X-ray)[28,35] according to Bird, and V_R=34.250 for CPD(MW), 40.109 for CPD(X-ray) according to Pozharskii with the normalization correction discussed above). V_R=26.377 for CPD(MW) is quite different from the value of 35 proposed in the earlier paper of Bird[23] for the completely localized Kekulé reference structure.

Molecular geometries of the five-membered heterocycles under study are taken mainly from the literature. Both experimental and theoretical geometries are included. MW

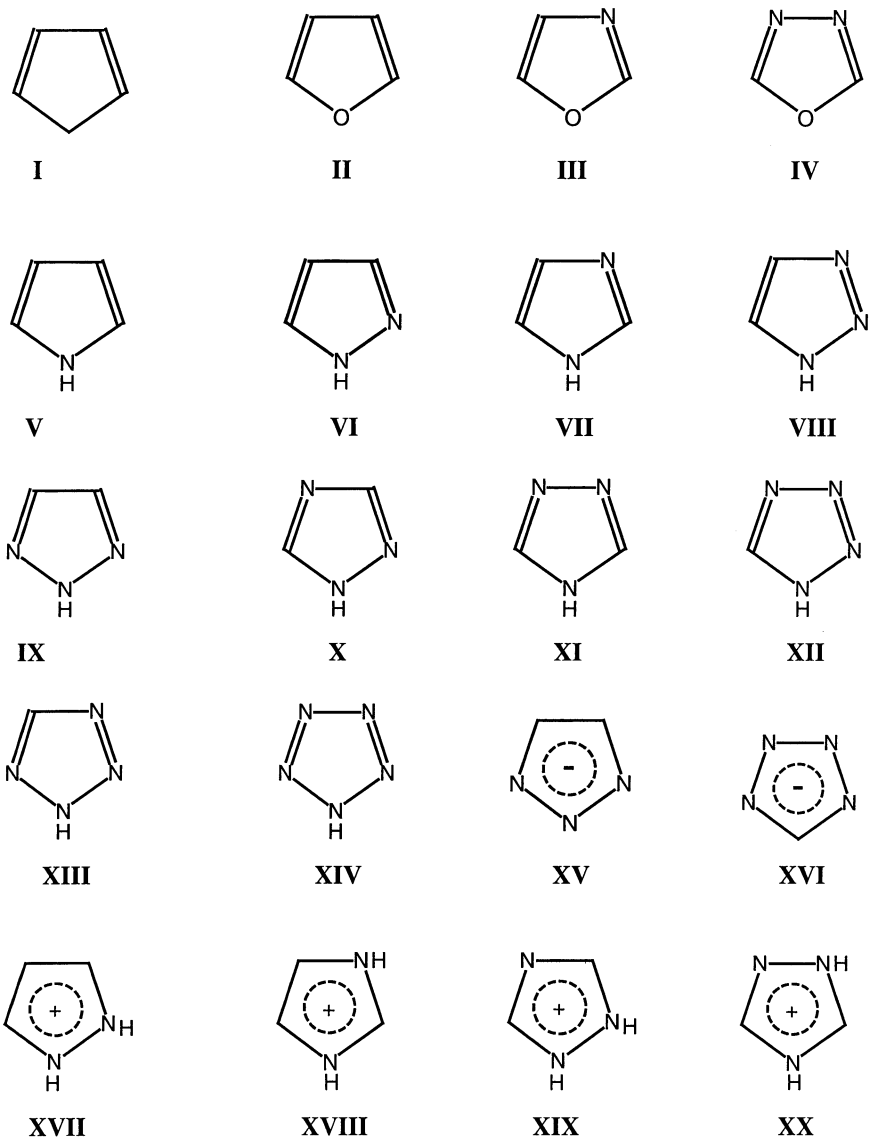

Figure 1. The five-membered ring systems under study: **I**, cyclopentadiene; **II**, furan; **III**, oxazole; **IV**, 1,3,4-oxadiazole; **V**, pyrrole; **VI**, pyrazole; **VII**, imidazole; **VIII**, *H*-1,2,3-triazole; **IX**, 2*H*-1,2,3-triazole; **X**, 1*H*-1,2,4-triazole; **XI**, 4*H*-1,2,4-triazole; **XII**, 1*H*-tetrazole; **XIII**, 2*H*-tetrazole; **XIV**, pentazole; **XV**, 1,2,3-triazolyl anion; **XVI**, tetrazolyl anion; **XVII**, 1*H*,2*H*-pyrazolium cation; **XVIII**, 1H,3*H*-imidazolium cation; **XIX**, 1*H*,2*H*-1,2,4-triazolium cation; **XX** 1*H*,4*H*-1,2,4-triazolium cation.

data are primarily from Ref. 29. The ab initio structures optimized at the SCF/6-31G level are taken mainly from Refs. 25, 37. The structures obtained at the higher 6-31G* level of the Hartree–Fock theory are taken primarily from the recent paper of Bean.[38] Molecular geometries optimized at the MP2/6-31G* level are additionally taken into consideration when available. In the case of 1,2,4-triazoles, our own MMX-M force field geometry is used, since the MW data is lacking. The MMX-M force field implemented in PCModel software[39] is found to work better for azole series compared with the express semi-empirical methods[25] at NDDO level, including the AM1 and PM3 approaches. The optimized geometry of 1*H*-1,2,4-triazole obtained with the MMX-M force field is as follows: $R_{NH-N(2)}$=1.41 Å, $R_{N(2)=C(3)}$=1.32 Å, $R_{C(3)-N(4)}$=1.36 Å, $R_{N(4)=C(5)}$=1.34 Å, and $R_{C(5)-NH}$=1.38 Å. For 4*H*-1,2,4-triazole, the bond lengths are R_{NH-C}=1.40 Å, $R_{C=N}$=1.32 Å, and R_{N-N}=1.35 Å.

3. Results and discussion

Table 2 presents the revised AI for the five-membered heterocycles under investigation. As evidenced by the data, the previously noted discrepancies between the two AI scales are indeed overcome. In particular, the fully refined AI values for the furan molecule with the geometry derived from the MW data closely match. The 32.2% value calculated according to the revised Bird scheme corresponds to the 30.3% value calculated by the revised scheme of Pozharskii. This is in sharp contrast with the original values of 43 and 12%, respectively. The AIs calculated by the modified Pozharskii scheme are much closer to the refined Bird values, if the normalization correction for the variation of mean BO, $\bar{N}$, is made. The remaining difference arises presumably from the difference between the arithmetic mean of the absolute values and the root-square-mean.

It is essential that the difference between the values of the two AI remains small to negligible over the whole range of compounds, from the highly localized oxadiazole to the highly delocalized pentazole and 2*H*-1,2,3-triazole. Therefore, any of the two refined AI systems, as well as their mixture or an average if necessary, can be used for characterization of the relative degrees of aromaticity, at least for the five-membered heterocycles with O and N heteroatoms.

It is further evident that the AIs obtained using X-ray derived structures with the MW derived CPD reference structure are quite different from the gas phase MW derived values. The indices are systematically lower for the H-bonding-free crystal structures than for the gas-phase structures. Moreover, in the cases of furan and 1*H*-1,2,4-triazole, where both room and cryogenic temperature X-ray structures are available, there exists a pronounced tendency for stronger bond localization with decreasing temperature. This trend, however, does not necessarily imply that aromaticity is decreased at low temperatures. The mean bond order, $\bar{N}$, drastically increases on cooling, since bonds become shorter. Unfortunately, there are not enough data to verify the generality of this trend.

The reverse order of AIs, i.e. AI(X-ray)>AI(MW), is observed for H-bonded pyrazole and imidazole with unsubstituted NH. For comparison, *N*-substituted 2*H*-1,2,3- and 4*H*-1,2,4- triazoles do not form H-bonds in crystal phase and, as a consequence, do not reverse the order of AIs. It is reasonable to assume that strong hydrogen bonding in crystals may lead to the extra delocalization of the peripheral bonds in the heterocycles, presumably due to the higher symmetry of the ring in crystal phase. In the isolated molecules, a formally double bond is created by the pyridine-like nitrogen atom, and a formally single bond is created by the pyrrole-like nitrogen atom. In crystal state, both types of nitrogen atoms are involved in the H-bonding network and are less distinct. The corresponding peripheral bonds are characterized by intermediate orders between the single and the double bonds.

The possible influence of the H-bond interaction in the crystal lattice on the bond lengths was indicated earlier in the papers of Krygowski.[5,61] Later, an attempt was made by Katritzky, Karelson, and Wells[12] to investigate the effect more closely within azole series. The results, in particular for pyrazole, were rather ambiguous, partly because the conventional Bird and Pozharskii indices were used.[12] In our study, pyrazole (**VI**) does not reveal any deflection from the common trend for H-bonded crystal structures. Unfortunately, the room temperature X-ray structure[48] for free-NH imidazole (**VII**) appears inadequate. The C4–C5 bond of 1.311 Å is likely too short and mean BO is excessively large. The MW structure[54] for 1*H*-1,2,4-triazole (**X**) has similar problems as discussed earlier in the literature.[47] A proper comparison of the counterparts is hardly possible in these two cases.

An interesting question arises concerning the extra bond localization observed in crystals for the 'normal', not H-bonded X-ray structures relative to the gas phase structures. Can the extra bond localization be fully counterbalanced by use of the X-ray CPD as a reference? Based on the data of Table 2, the answer is no, even though in a few cases, including furan in FDCA, oxazole in POPOP and oxadiazole in PPD, the X-ray/X-ray AI values closely approximate the gas phase/MW results. It is important to remember that the reference CPD X-ray structure is obtained at a deep cryogenic temperature of −150°C, while the sample geometries are derived at room temperature. When the X-ray data are available for both the sample and reference structures at the same temperature, as in the case of furan or, in part, 2*H*-1,2,3-triazole, the solid state/X-ray AI remains still substantially lower than the gas phase/MW AI. This result implies that not only the uniformity of bond order, but also effective aromaticity may decrease in the solid state.

Now, with refined AIs as a tool, several trends in the dependence of the aromaticity on the chemical structure of the five-membered heterocycles become more distinct. The cycles with oxygen appear less aromatic than their nitrogen-bearing analogs. Compare furan with pyrrole, oxazole with imidazole, and 1,3,4-oxadiazole with 4*H*-1,2,4-triazole. This trend is in good agreement with both the observed reactivity and theoretical predictions.[1,2,6,13,22,62,63] Perhaps, the best illustration is the highly divergent valence state ionization potential (VSIP) values for the pyrrole-like heteroatoms, −32.9 and −21.0 eV for oxygen and nitrogen, respectively.[64]

In order to clarify the details of the aromaticity–structure relationship, it is highly desirable that the geometry for all the molecules under study is derived by the same theoretical or experimental approach. Among the data of Table 2, the AI values calculated for ab initio optimized geometries are represented best. Table 3 contains the AIs for the azole series calculated for ab initio optimized structures at the different levels of theory. Quantitatively, rather distinct AI values are obtained for the SCF/6-31G optimized geometries, on the one hand, and for the correlated geometries at the MP2/6-31G* level, on the other. In most cases, with a possible exception of anions, the account for electron correlation at the MP2 level results in much more uniform peripheral bond orders compared to the geometries obtained at the SCF level. The effect is indeed due to electron correlation, and not the expansion of the basis set from 6-31G to 6-31G*. This is evident for pyrrole, imidazole, two 1,2,4-triazoles, two tetrazoles, pentazole, and 1*H*,3*H*-imidazolium cation, where both 6-31G and 6-31G* SCF optimized geometries are available. Except for pyrazole, the polarization function alone has a minor effect on the AIs. Still, this secondary effect is of the same sign as the electron correlation effect. Peripheral bond orders are more uniform for the larger basis set. At the same time, the mean bond order, $\bar{N}$, evaluated from the Gordy relationship (1), is substantially lower for the correlated structures compared to the SCF structures. In the light of the recent study by Krygowski and Cyranski[36] this result may imply that the aromaticity increase at the MP2 level of theory over the SCF values is less significant than may be concluded based solely on the AI values.

Comparison of the SCF and MP2 results to one another and with the AIs calculated from the experimental geometries gives rise to the following question. Are the MP2 correlated geometries indeed so good in predicting the gas phase

Table 2. AIs for the CPD (**I**) and five-membered heterocycles (**II**–**XX**) calculated according to Bird and Pozharskii with CPD by MW as a reference structure

Cycle no.	Method of geometry determination	References	Bond order averaged over the ring, $\bar{N}$[a]	AIs calculated according to		
				Pozharskii		Bird
				Unnormalized	Normalized for $\bar{N}$ variation	
I	MW	29	1.4978	0	0	0
	X-ray (at −150°C)	28,35	1.6126	−26.1 (0)	−17.0 (0)	−12.9 (0)
II	MW	29	1.5408	28.3	30.3	32.2
	X-ray (in FDCA)[b]	28	1.5364	20.6 (37.0)	22.6 (33.9)	23.9 (32.6)
	X-ray (below −150°C)	40	1.6241	−2.2 (18.9)	5.8 (19.5)	7.5 (18.1)
III	MW	41	1.5454	17.2	19.8	20.6
	X-ray (in POPOP)[c]	28	1.5490	14.0 (31.8)	16.8 (29.0)	19.1 (28.4)
IV	Gas electronogr. (for PPD)[d]	42	1.5184	23.6	24.6	25.3
	X-ray (in PPD)	43	1.5508	9.9 (28.5)	12.9 (25.7)	11.4 (21.6)
	X-ray (in substd. PPD)	43	1.5231	6.4 (25.8)	7.9 (21.4)	5.0 (15.9)
V	MW	29	1.6048	70.9	72.8	73.0
	6-31G	37	1.6283	56.4	59.9	57.8
	MP2/6-31G*	44	1.6027	69.0	71.0	71.4
VI	MW	37,45	1.6154	66.9	69.3	71.0
	X-ray (form A)[e]	28,46	1.6903	73.4 (78.9)	76.4 (79.9)	75.2 (78.0)
	X-ray (form B)[e]	28,46	1.6877	72.2 (78.0)	75.3 (78.9)	76.6 (79.3)
	6-31G	37	1.6429	59.9	63.5	65.3
	MP2/6-31G*	25,47	1.5980	76.5	78.0	79.1
VII	MW	25,41	1.6140	53.6	57.0	57.9
	X-ray (room temperature)[e]	28,48	1.7199	28.9 (43.6)	38.1 (47.1)	41.2 (47.9)
	X-ray (at −150°C)[e]	28,49	1.6360	57.0 (65.9)	60.6 (66.4)	63.5 (67.5)
	Neutron diffr. (at −170°C)[e]	50	1.6335	62.1 (70.0)	65.3 (70.3)	67.6 (71.3)
	Neutron diffr. (corr. to room temperature)[e]	50	1.5703	60.6 (68.8)	62.4 (67.9)	65.0 (69.0)
	6-31G	37	1.6296	45.5	49.9	50.7
	MP2/6-31G*	44	1.5977	64.9	67.1	67.2
VIII	X-ray (aver.)	51	1.5827	70.4 (76.6)	72.0 (76.1)	71.1 (74.4)
	MP2/6-31G*	47,52	1.5762	74.6	75.8	75.9
IX	MW	25,51	1.6086	95.4	95.7	95.8
	X-ray (aver.)	51	1.6019	85.8 (88.8)	86.8 (88.7)	86.8 (88.3)
	MP2/6-31G*	52,53	1.5903	87.1	87.9	88.1
X	MW	25,54	1.6217	32.6	37.7	41.8
	X-ray (room temperature)[e]	28,55	1.5928	75.4 (80.5)	76.8 (80.2)	77.4 (80.0)
	X-ray (at −160°C)[e]	28,56	1.6370	64.3 (71.7)	67.4 (72.1)	67.9 (71.6)
	6-31G	37	1.6415	49.6	54.0	57.0
	MP2/6-31G*	47	1.5951	72.5	74.2	76.2
XI	MMX-M	–[f]	1.5190	43.8	44.6	47.9
	X-ray (in PPZ)[g]	57	1.5688	41.5 (53.6)	44.2 (52.3)	45.5 (51.7)
	6-31G	37	1.6254	31.1	36.5	38.4
	MP2/6-31G*	47	1.5754	52.0	54.4	55.7
	MMX-M	–[f]	1.5356	48.2	49.5	49.9
XII	X-ray	38	1.6619	47.6 (58.5)	52.9 (59.8)	55.2 (60.3)
	X-ray[e]	58	1.6868	66.0 (73.0)	69.8 (74.2)	70.6 (74.0)
	6-31G	25,37	1.6361	40.3	45.3	48.4
	MP2/6-31G*	58	1.5628	65.4	66.9	69.1
XIII	X-ray	38	1.6704	67.2 (74.0)	70.6 (74.9)	71.4 (74.7)
	6-31G	25,37	1.6249	67.1	69.7	70.5
	MP2/6-31G*	58	1.5713	86.7	87.3	88.3
XIV	6-31G	25,37	1.6478	53.5	57.7	57.7
	MP2/6-31G*	47	1.5454	91.2	91.4	89.9
XV	MP2/6-31G*	59	1.5257	70.0	70.5	71.3
XVI	X-ray (as Na^+ salt)	60	1.6046	68.8 (75.2)	70.9 (75.1)	71.1 (74.4)
	MP2/6-31G*	58	1.5070	73.3	73.5	73.8
XVII	6-31G	25,37	1.6538	78.0	80.0	75.3
XVIII	6-31G	25,37	1.6474	41.0	46.3	47.7
	MP2/6-31G*	44	1.6173	65.2	67.8	68.8

Table 2. (*continued*)

Cycle no.	Method of geometry determination	References	Bond order averaged over the ring, $\bar{N}$[a]	AIs calculated according to		
				Pozharskii		Bird
				Unnormalized	Normalized for $\bar{N}$ variation	
XIX	6-31G	25,37	1.6567	75.5	77.8	72.8
XX	6-31G	25,37	1.6560	44.0	49.5	51.6

For the structures from X-ray data, an additional value in parentheses is given obtained in the same manner with CPD by X-ray as a reference.
[a] Average of the BOs calculated from the Gordy relationship (1) with the *a* and *b* values determined in this work.
[b] Furan-2,5-dicarboxylic acid.
[c] 1,4-Bis[2-(5-phenyl)oxadiazolyl]benzene.
[d] 2,5-Diphenyl-1,3,4-oxadiazole.
[e] H-bonded structures in the crystal phase.
[f] This work.
[g] 3,4,5-Triphenyl-4*H*-1,2,4-triazole.

structures in the azole series as is often believed?[47,52,58,59] A closer examination reveals that the situation is neither so unequivocally optimistic as claimed in the paper of El-Bakali Kassimi, Doerksen, and Thakkar,[47] nor so obscure as it appears from the treatment of Ostrovskii, Yerusalimskii, and Scherbinin.[25] Two problems should be distinguished. The first one is the proper evaluation of the mean bond lengths and, as a sequence, bond orders. The second one concerns the theoretical prediction of the AIs that are used as a criterion of the bond orders divergence.

The first problem beyond any doubt is solved better at the MP2 level of theory than within Hartree–Fock approximation, see, for example, Ref. 47 and references therein. As seen from the Tables 2 and 3, the mean bond orders derived from the MP2 optimized geometries in most cases (except for tetrazoles) are much closer to the experimental $\bar{N}$ than the corresponding SCF values. On the other hand, the account for the electron correlation at the second order does not have substantial advantages over SCF in reproducing the relative experimental bond variations estimated by AIs. In some cases, the approximate treatment of electron correlation makes worse predictions.

Table 4 summarizes the agreement achieved between the AIs calculated for ab initio optimized and experimental geometries within the azole series. The results clearly indicate that the experimental MW values are better reproduced at the SCF level of theory rather than at the MP2 correlated level. Moreover, in the two cases where both the MP2 and the superior QCISD structures are available, i.e. for pyrazole and 1*H*-tetrazole, see Table 3, the AI values derived from QCISD are closer to the SCF rather than MP2 values. In the case of hydrogen pentazole, the high-level correlated geometry is available from the CCSD treatment of Ferris and Bartlett.[65] Again, the corresponding AI of 73.8 falls between the lower SCF/6-31G* value of 70.1 and the higher MP2/6-31G* value of 90.7, closer to the SCF value.

The AI calculated with the experimental geometry of 4*H*-1,2,4-triazole derived from the X-ray spectral data in the H-nonbonded 3,4,5-triphenyl form better fits to the SCF value, when CPD(MW) is taken as the reference structure. If CPD(X-ray) is used, better agreement with the MP2 value is achieved. For 1*H*-tetrazole, when both H-bonded and H-nonbonded X-ray geometries are available, the first one gives the AI closer to the MP2 value while the second structure provides the AI better reproduced at the Hartree–Fock level of theory. The AIs of the rest azoles in their experimental X-ray geometries are closer to the MP2/6-31G* values. In all these cases, the H-bonded crystal structures are the only ones available from the literature.

Therefore, molecular geometries correlated at the MP2 level of theory, indeed, can be superior over SCF optimized geometries in predicting the bond order uniformity within the azole series. Their predictive power, however, is restricted to the H-bonded crystal structures rather than to the free molecules. This is due to the extra delocalization in the H-bonded environment as discussed above. Otherwise, SCF optimized geometries or those obtained at the levels of theory that are higher than MP2, including MP4, QCISD, CCSD, etc., are preferable.

Note that in the case of azolyl anions **XV** and **XVI**, MP2 provides AIs whose values are lower than the SCF values. The parent cyclopentadienyl anion is well-known to be fully delocalized at the SCF level of theory. It is unlikely that the high degree of bond delocalization observed in anionic systems depended upon electron correlation effects in the same manner as it does in neutral azole molecules.

Next, consider the dependence of AIs on the presence and mutual position of the pyrrole- and pyridine-like heteroatoms in the cycle within the azole series. The data are presented in the Table 5. At the SCF level, replacement of the carbon atom at the α position relative to the NH group with pyridine-like nitrogen atom increases the AI of the neutral molecule. Compare e.g. (6-31G* vs 6-31G): (79.7/–) for 2*H*-1,2,3-triazole>(70.4/64.4) for pyrazole>(60.7/58.9) for pyrrole; (77.4/70.1) for 2*H*-tetrazole>(59.7/55.5) for 1*H*-1,2,4-triazole>(51.7/50.3) for imidazole; (77.4/70.1) for 2*H*-tetrazole>(68.4/–) for 1*H*-1,2,3-triazole>(51.7/50.3) for imidazole; (70.1/–) for pentazole>(54.5/46.9) for 1*H*-tetrazole>(40.9/37.5) for 4*H*-1,2,4-triazole. On the contrary, the same replacement made at the β position reduces the AI. Compare (40.9/37.5) for 4*H*-1,2,4-triazole<(51.7/50.3)

Table 3. AIs calculated for the azole series using ab initio geometries optimized at different levels of theory. The values obtained with the most reliable experimental geometries are given for comparison
=?^ Table 3. (*continued*)

Molecule	SCF/6-31G	AIs for the level of theory			Experiment
		SCF/6-31G*[a]	MP2/6-31G*	Other	
V, pyrrole	58.9 [1.6283][b]	60.7 [1.6663]	71.2 [1.6027]	–	72.9[c] [1.6048]
VI, pyrazole	64.4 [1.6429]	70.4 [1.6230]	78.6 [1.5980]	71.6[d] [1.6023]	70.2[c] [1.6154]
VII, imidazole	50.3 [1.6296]	51.6 [1.6947]	67.2 [1.5977]	–	57.5[c] [1.6140]
VIII, 1*H*-1,2,3-triazole	–	68.4 [1.7256]	75.9 [1.5762]	50.0[e] [1.6033]	71.6 (75.3)[f] [1.5827]
IX, 2*H*-1,2,3-triazole	–	79.7 [1.7441]	88.0 [1.5903]	63.8[e] [1.6152]	95.8[c] [1.6086]; 86.8 (88.5)[f] [1.6019]
X, 1*H*-1,2,4-triazole	55.5 [1.6415]	59.7 [1.7302]	75.2 [1.5951]	76.9[g] [1.6056]	77.1 (80.1)[f,h] [1.5928]; 67.7 (71.9)[f,i] [1.6370]
XI, 4*H*-1,2,4-triazole	37.5 [1.6254]	40.9 [1.7144]	55.1 [1.5754]	–	44.9 (52.0)[f] [1.5688]
XII, 1*H*-tetrazole	46.9 [1.6361]	54.5 [1.7504]	68.0 [1.5628]	68.3[j] [1.5747]; 55.5[k] [1.5869]	54.0 (60.1)[f] [1.6619]; 70.2(74.1)[f] [1.6868]
XIII, 2*H*-tetrazole	70.1 [1.6249]	77.4 [1.7641]	87.8 [1.5713]	–	71.0 (74.8)[f] [1.6704]
XIV, pentazole	57.7 [1.6478]	70.1 [1.7861]	90.7 [1.5454]	69.8[l] [1.7725]; 91.5[m] [1.5154]; 73.8[n] [1.5780]	–
XV, 1,2,3-triazolyl anion	–	–	70.9 [1.5257]	89.2[o] [1.6611]	–
XVI, tetrazolyl anion	–	78.2 [1.7163]	73.7 [1.5070]	–	71.0 (74.8) [1.6046][f]
XVII, 1*H*,2*H*-pyrazolium cation	77.7 [1.6538]	–	–	–	–
XVIII, 1*H*,3*H*-imidazolium cation	47.0 [1.6474]	49.3 [1.6998]	68.3 [1.6173]	–	–
XIX, 1*H*,2*H*-1,2,4-triazolium cation	75.3 [1.6567]	–	–	–	–
XX, 1*H*,4*H*-1,2,4-triazolium cation	50.6 [1.656]	[1.6560]	–	–	–

Arithmetic means of the refined Bird and Pozharskii values are presented.
[a] Refs. 38, 44 and 58.
[b] The mean bond order values are given in the square brackets.
[c] MW gas phase geometry, see Table 2.
[d] QCISD/6-31G**.[47]
[e] SCF/DZ(7s,3p).[51]
[f] X-Ray data structure, see Table 2.
[g] MP2/6-311G**.[47]
[h] Room temperature[55]
[i] At −160°C.[56]
[j] MP2/6-311G(2d,2p).[58]
[k] QCISD/6-31G*.[58]
[l] SCF/DZP.[65]
[m] MBPT(2)/DZP.[65]
[n] CCSD.[65]
[o] SCF/4-21G* (N*).[59]

Table 4. Agreement between AIs calculated for the experimental and theoretical geometries within the azole series

Molecule	Experimental procedure	Better reproduced at the level of theory	
		SCF[a]	MP2[b]
VI, pyrazole	MW	+	
VII, imidazole	MW	+	
X, 1*H*-1,2,4-triazole	MW	+	
VI, pyrazole	X-ray (H-bonded)		+
VII, imidazole	X-ray (H-bonded)		+
X, 1*H*-1,2,4-triazole	X-ray (H-bonded)		+
XII, 1*H*-tetrazole	X-ray (H-bonded)		+
	X-ray (not H-bonded)	+	
XIII, 2*H*-tetrazole	X-ray (not H-bonded)	+	
XI, 4*H*-1,2,4-triazole	X-ray (not H-bonded)	+ (relative to CPD(MW))	+ (relative to CPD(X-ray))
VIII and **IX**, two 1,2,3-triazoles	X-ray (averaged over the range of H-bonded and not H-bonded structures)	Intermediate	

[a] SCF/6-31G.
[b] MP2/6-31G*.

for imidazole<(60.7/58.9) for pyrrole; (54.5/46.9) for 1*H*-tetrazole<(59.7/55.5) for 1*H*-1,2,4-triazole<(70.4/64.4) for pyrazole; (54.5/46.9) for 1*H*-tetrazole<(68.4/–) for 1*H*-1,2,3-triazole<(70.4/64.4) for pyrazole; (70.1/57.7) for pentazole<(77.4/70.1) for 2*H*-tetrazole<(79.7/–) for 2*H*-1,2,3-triazole. When both α and β positions are substituted with pyridine-like nitrogen atoms, their effects tend to compensate one another. For example, pentazole (70.1/57.7)≈1*H*-1,2,3-triazole (68.4/–); 1*H*-1,2,4-triazole (59.7/55.5)≈pyrrole (58.9); 2*H*-tetrazole (77.4/70.1)≥pyrazole (70.4/64.4); 1*H*-tetrazole (54.5/46.9)≈imidazole (51.7/50.3). The AI of protonated azoles **XVII**–**XX** depends mainly on the mutual position of two NH groups. The location of the free pyridine-like nitrogen atom is of minor importance in this case. The AIs diverge much more between the azolium cations of 'pyrazolic' and 'imidazolic' structures, compounds **XVII** and **XVIII**, **XIX** and **XX**, respectively, than in the pairs **XVII** and **XIX**, **XVIII** and **XX**.

These tendencies are reproduced, with few exceptions, at the MP2/6-31G* correlated level of theory as well. So, for the α substitution: 2*H*-1,2,3-triazole (88.0)>pyrazole (78.6)>pyrrole (71.2); 2*H*-tetrazole (87.8)>{1*H*-1,2,3-triazole (75.9), 1*H*-1,2,4-triazole (75.2)}>imidazole (67.2); pentazole (90.7)>1*H*-tetrazole (68.0)>4*H*-1,2,4-triazole (55.1). For the β substitution: 4*H*-1,2,4-triazole (55.1)<imidazole (67.2)<pyrrole (71.2); 1*H*-tetrazole (68.0)<{1*H*-1,2,3-triazole (75.9), 1*H*-1,2,4-triazole (75.2)}≤pyrazole (78.6); pentazole (90.7)>2*H*-tetrazole (87.8)≈2*H*-1,2,3-triazole (88.0). When both substitutions are made simultaneously, the effect of the α substitution prevails, e.g. 1*H*-1,2,3-triazole (75.9), 1*H*-1,2,4-triazole (75.2)}>pyrrole (71.2); 1*H*-tetrazole (68.0)≈imidazole (67.2); 2*H*-tetrazole (87.8)>pyrazole (78.6); pentazole (90.7)>{1*H*-1,2,3-triazole (75.9), 1*H*-1,2,4-triazole (75.2)}. The relative 'power' of the two positions is not the same at the MP2 correlated level. This result that requires further verification in the light of the above discussion of the strengths and weaknesses of SCF and MP2 theories.

Finally, compare the relative aromaticities of the structural

Table 5. Relative aromaticities of azoles as a function of the number and location of pyridine-like nitrogen atoms in the cycle evaluated for SCF and MP2 optimized geometries

The number of pyridine-like atoms	Molecule	Position(s) of the pyridine-like atom(s)	The level of theory		
			SCF[a]		MP2[b]
			6-31G	6-31G*	6-31G*
0	Pyrrole	–	58.9	60.7	71.2
1	Pyrazole	α	64.4	70.4	78.6
	Imidazole	β	50.3	51.7	67.2
2	2*H*-1,2,3-triazole	α, α′	(63.8)[c]	79.7	88.0
	1*H*-1,2,3-triazole	α, β	(50.0)[c]	68.4	75.9
	1*H*-1,2,4-triazole	α, β′	55.5	59.7	75.2
	4*H*-1,2,4-triazole	β, β′	37.5	40.9	55.1
3	2*H*-tetrazole	α, α′, β	70.1	77.4	87.8
	1*H*-tetrazole	α, β, β′	46.9	54.5	68.0
4	Pentazole	α, α′, β, β′	57.7	70.1	90.7

Arithmetic means of the refined Bird and Pozharskii values are presented.
[a] SCF/6-31G.
[a] MP2/6-31G*.
[b] SCF/DZ(7s,3p)[51] values.

Table 6. Reference single and double bond lengths in Å used in HOMA and AI calculations

Bond	$R(1)$			$R(2)$		
	HOMA[a]	AI		HOMA[a]	AI	
		Bird[b]	This work		Bird[b]	This work
C–C	1.467	1.584	1.538	1.349	1.354	1.338
C–N	1.465	1.470	1.472	1.269	1.273	1.285
C–O	1.367	1.420	1.425	1.217	1.222	1.212
C–S	1.807	1.821	1.827	1.611	1.610	1.599
N–N	1.420	1.480	1.450	1.254	1.244	1.251
N–O	1.415	1.426	1.463	1.164	1.201	1.210

[a] Refs. 5 and 20.
[b] Bond lengths consistent with the Gordy relationship with original *a* and *b*, see Refs. 23 and 26.

isomers with the same number of nitrogen atoms. The first isomer has 'pyrazolic', while another has 'imidazolic' arrangement of the pyridine-like nitrogen atom relative to the pyrrole-like atom, e.g. pyrazole vs. imidazole, 2*H*- vs. 1*H*-1,2,3-triazoles and tetrazoles, 1*H*- vs. 4*H*-1,2,4-triazole. As follows from the general trend just specified, all the pyrazolic structures should be much more aromatic than their imidazolic counterparts, both at the SCF and at the correlated levels of theory. Table 5 proves this true in every case. This observation is firmly supported by the chemical behavior[59] of the azole series.

Derivation of the regularities in the oxazole series is a more challenging problem, since the characteristics of the N–O bond are much poorer defined. We have re-evaluated the *a* and *b* constants in the Gordy relationship for the N–O bond from the crystallographic data.[30] With these parameters we have calculated the AIs for some oxazoles. Molecular geometries optimized at the SCF/6-31G* level are available from the paper of Bean.[38] The obtained averaged AI values are: furan, 27.4; isoxazole, 32.8; oxazole, 18.5; 1,2,3-oxadiazole, 25.6; 1,2,4-oxadiazole, 25.9; 1,2,5-oxadiazole, 35.0; 1,3,4-oxadiazole, 10.4; 1,2,3,4-oxatriazole, 16.9; 1,2,3,5-oxatriazole, 29.7; oxatetrazole, 17.5.

It is evident from these data that all members of the oxazole series have much more localized structures and exhibit much less aromaticity compared to the corresponding analogues from the azole series. Also, the AIs within the oxazole series vary within a far narrower range. Nevertheless, if we consider the dependence of AI upon the mutual position of the 'pyrrole-like' oxygen atom and the 'pyridine-like' nitrogen atoms, the regularities closely resemble those just specified for the azoles. AI gradually rises with the number of α aza substitutions, i.e. from furan via isoxazole to 1,2,5-oxadiazole and from oxazole via 1,2,3- and 1,2,4-oxazoles up to 1,2,3,5-oxatriazole. On the other hand, AI drops in all β aza derivatives, i.e. from furan via oxazole to 1,3,4-oxadiazole and from isoxazole via 1,2,3- and 1,2,4-oxazoles down to 1,2,3,4-oxatriazole. When both α and β substituents are present, the effect of the β substitution dominates in oxazole series, in contrast to the azoles. AI decreases from furan via 1,2,3- and 1,2,4-oxazoles down to oxatetrazole. Note that with the *a* and *b* parameters for the N–O bond proposed by Gordy no regularities in the α substituted oxazole series could be detected.

Unfortunately, we are not aware of any consistent experimental reports on the relative aromaticities of oxazoles to be compared with the AI predictions. Nevertheless, semi-empirical aromatic stabilization energies (ASE) calculated as the energetic effect of an imaginary homodesmotic hydrogenation reaction are available from the paper of Katritzky et al.[66] These values are given below (in kcal mol^{-1}): furan, 19.8; 1,3-oxazole, 18.1; 1,3,4-oxadiazole, 13.3; izoxazole, 24.1; and 1,2,5-oxadiazole, 26.4. The order is the same for both ASE and AI values. Moreover, a good linear correlation is found between two sets, with R=0.9445 and SD=1.4082. (Note that ASE were obtained with molecular geometries optimized at MP2/6-31G* level.) We may conclude that the modified AIs form an appropriate tool for prediction of the relative aromatic stabilization energies in such cases.

Recently, Mrozek, Karolak–Wojciechowska, Amiel, and Barbe (MKWAB)[67] applied the HOMA index to crystallographic data taken from the Cambridge Structural Database in order to derive regularities governing aromaticities of the five-membered heterorings with nitrogen, sulphur, or oxygen. Based on a multitude of structures considered in this study, one general trend regarding aromaticity in the azole series has been detected. Namely, the aromaticity gradually increases with increasing number of heteroatoms. Among other things, imidazole is treated by MKWAB as much more aromatic than pyrrole, 4*H*-1,2,4-triazoles as more aromatic than the 1*H* tautomers, and so forth. Similar conclusions can be made from the earlier study with the HOMA index by the Krygowski group.[20] Since these observations are in conflict with our results, we inspected this point more closely.

First, note that our approach does not average over the available crystal structures. Also, it is not clear, if a good correlation may be expected in general between the AIs calculated according to Bird, Pozharskii, or the modified scheme and the HOMA values. The HOMA index as defined by Krygowski and Cyranski[20] consists of two contributions to the overall aromaticity, EN and GEO, respectively

$$\begin{aligned} \mathrm{HOMA} &= \mathrm{EN} - \mathrm{GEO} \\ &= 1 - \alpha(R_{\mathrm{opt}} - R_{\mathrm{av}})^2 - \frac{\alpha}{\mathrm{N}} \sum_i (R_{\mathrm{av}} - R_i)^2 \end{aligned} \tag{7}$$

These terms were obtained through the splitting of the initial harmonic oscillator model index. The GEO term corresponds to the decrease of aromaticity due to bond alternation. The EN term describes dearomatization due to bond elongation. The GEO term is related to AI while the EN contribution does not correlate with AI and is supposed to deal with other types of aromaticity, including magnetic properties. α and R_{opt} in Eq. (7) are empirical parameters characterizing individual bond types. R_{av} denotes the bond length averaged over the cycle.

The harmonic oscillator model is designed to characterize the resonance stabilization energy of a system relative to benzene. To built HOMA lengths of the single and double

Table 7. Modified AIs compared to HOMA values and HOSE resonance energies

Molecule	Aromaticity indices						HOSE Resonance energies, kcal mol^{-1}		
	HF/6-31G*[a]		Experimental[a]				Dewar	Total (scaled)	Experimental[b]
	AI	1-GEO	AI	HOMA					
				1-GEO	EN×10^2	total			
V, pyrrole	60.7	0.799	72.9	0.942	3.75	0.905	5.240 (0.434)	34.52 (0.754)	34.8 [25.5];[c] [25.68][d]
VI, pyrazole	70.4	0.904	70.2	0.922	2.98	0.892	6.993 (0.579)	34.84 (0.761)	[25.80][d]
VII, imidazole	51.6	0.832	57.5	0.882	1.41	0.868	4.862 (0.402)	28.94 (0.632)	40.0? [25.21];[c] [23.76][d]
VIII, 1*H*-1,2,3-triazole	68.4	0.903	71.6	0.913	3.06	0.882	7.609 (0.630)	32.11 (0.701)	–
IX, 2*H*-1,2,3-triazole	79.7	0.967	86.8	0.968	2.73	0.941	13.540 (1.121)	45.37 (0.991)	–
X, 1*H*-1,2,4-triazole	59.7	0.912	67.0[e]	0.936	3.05	0.905	7.336 (0.607)	32.75 (0.715)	[26.2];[c] [23.88][d]
XI, 4*H*-1,2,4-triazole	40.9	0.797	44.9	0.820	6.65	0.754	3.308 (0.274)	23.51 (0.513)	–
XII, 1*H*-tetrazole	55.8	0.856	54.0	0.873	0.337	0.870	7.538 (0.624)	31.78 (0.694)	[27.4];[c] [26.04][d]
XIII, 2*H*-tetrazole	78.3	0.967	71.0	0.946	0.0457	0.946	10.418 (0.862)	37.58 (0.821)	–
XIV, pentazole	70.6	0.923	–	–	–	–	–	–	[10.8?][d]

The reduced values relative to the resonance energy of benzene (12.083 and 45.8 kcal mol^{-1} for DRE and TRE, respectively) are given in parentheses.
[a] The source of the molecular geometry.
[b] The values in square brackets are aromatic stabilization energies (ASE).
[c] Reference 66.
[d] Reference 71.
[e] An artificial geometry obtained by replacing abnormally short N(1)–C(5) bond in the crystal structure by the value of 1.361 Å typical for *meso*-diazoles.

bonds were referenced. The lengths of several reference bonds are collected in the Table 6 and compared with the two sets of the bond lengths used to derive the Gordy relationship. The data of Table 6 indicate that HOMA is based upon the single and double bonds typical for conjugated diene molecules rather than upon the isolated single and double bonds. In contrast to the HOMA index, AI is originally based on bond orders rather than bond lengths. To relate to the bond orders the reference is taken to the isolated bonds. The reference bond length values that are employed here are very close to those used by Bird in his later paper[67] calculating resonance energies from molecular dimensions. The set used by Gordy corresponds to neither conjugated nor isolated bonds and contains sharp outliers.

Besides the difference in the reference bond lengths, two other sources of discrepancy between the predictions of the AI and HOMA indices should be mentioned. First, consider the EN contribution to HOMA. Since the HOMA index deals with reference bond lengths, not bond orders, the HOMA values strongly depend via the EN term on the source of the geometric structure. Most of the HOMA results are obtained with crystal structures from CSD rather than with gas phase molecular dimensions.

Second, every type of bond enters HOMA with its own weighting factor α, dependent on the stretching/shortening force constant. In particular, the α(C–C) value is taken[5,20] to be twice as large as α(N–N) and nearly three times as large as α(C–N). This weighting implies that the dearomatization of the cycle due to the N–N and C–N bond localization is less pronounced than that due to the C–C bond localization. This may result in extra enhancement in the HOMA values for imidazoles and polyaza cycles relative to pyrrole, explaining the increase of aromaticity with the number of aza groups observed by Krygowski and MKWAB.

In order to evaluate the role of these factors, we have calculated the HOMA values for pyrrole and azoles **I**–**XIV** with the geometries from the ab initio SCF/6-31G* calculations of Bean[38] and with the experimental geometries available from the literature. The experimental geometries are the same as before, see Table 3. The set of parameters α(X−Y), R_{opt}, and reference bond lengths $R(1)$ and $R(2)$ are taken from the work of Krygowski and Cyranski.[5,20] To perform the averaging of the bond lengths over the cycle, different bonds are transformed into the virtual C–C, C–N, and N–N bonds as in Ref. 20, and the mean HOMA value are derived. The only distinction from their treatment is in avoiding crystallographic data.

The results are presented in Table 7 along with the corresponding AI values discussed above. For the experimental geometries, the overall HOMA values as well as their decomposition into the EN and GEO terms are given. In the case of the SCF/6-31G* geometries, the EN contribution analysis is not appropriate, because of the large errors in the mean bond lengths and bond orders at the Hartree–Fock level of theory (see Tables 2 and 3). Therefore, only the 1-GEO terms relative to AIs are given.

In addition to HOMA, direct evaluation of the resonance energies has been carried out for azoles based on the experimental molecular dimensions. The method used is due to

Table 8. Reference data used in the HOSE resonance energies calculations for the azole series

Bond	Bond lengths, Å						Force constants, dyn cm^{-1}		Constants in the formula (10) ($\times 10^4$ Pa)		Scaling factor[a]
	Conjugated			Isolated			$k(1)$	$k(2)$	A	B	
	$R(1)$	$R(2)$	R_{opt}[b]	$R(1)$	$R(2)$	R_{opt}					
C–C	1.469	1.342	1.394	1.534	1.338	1.418	4.5	9.6	44.42	26.02	1.335
C–N	1.430	1.290	1.347	1.472	1.285	1.361	4.9	10.5	48.98	29.95	1.279
N–N	1.420	1.254	1.316	1.450	1.251	1.326	3.55	10.0	50.60	32.45	1.289

[a] Introduced to adjust the calculated TRE values with the experimental values for the reference structures, see text.
[b] 'Optimal' bond length. For $R>R_{opt}$, single bond constants are used; for $R<R_{opt}$, double bond constants are used.

Bird.[68] It is based upon the harmonic oscillator stabilization energy (HOSE) concept[69] of Krygowski et al. and is related to HOMA. The resonance energy is calculated as the energy of deformation necessary to transform a cyclic molecule into its Kekule structure with localized single and double bonds. The returning force on the shortened single bond F is proportional in the HOSE model to the bond length difference

$$F = -k(1)|R - R(1)| \tag{8}$$

with a similar expression for the stretching of the double bond. In the simplest approximation,[68] the force constant is independent of R, and the resonance energy contribution from an individual bond is

$$E_{def} = -\tfrac{1}{2}k(R - R_0)^2 \tag{9}$$

where R_0 stands for either $R(1)$ or $R(2)$ and R stands for the length of stretched/shortened bond. However, a typical force constant decreases with bond elongation. The decrease may be expressed in a linear form

$$k = A + BR \tag{10}$$

Therefore, it is not clear what kind of force constant ($k(1)$, $k(2)$, or $k(R)$) is an appropriate choice for use in the formula like Eq. (9). Bird, in his study,[68] has employed the $k(R)$ calculated from Eq. (10). Our tests show that this is only valid for R close to R_0. Otherwise, direct substitution of Eq. (10) into Eq. (8) is preferable with the final formula for the resonance energy

$$E_{def} = -\frac{1}{2}\left[k(i)X^2 + \frac{2}{3}BX^3\right]; \qquad i = 1 \text{ or } 2 \tag{11}$$

where X stands for $(R(i)-R)$; $X\geq 0$ for the shortened single bond and $X\leq 0$ for the stretched double bond. HOSE is defined as the negative value of E_{def} converted into kcal mol^{-1}, i.e.

$$\text{HOSE (kcal mol}^{-1}) = -E_{def} = 71.9766\left[k(i)X^2 + \frac{2}{3}BX^3\right], \tag{12}$$

and the aromatic stabilization energy is finally obtained via summation of the contributions from individual bonds. The resulting value corresponds to either Dewar type resonance energy (DRE) or total resonance energy (TRE)[68] depending on weather the conjugated or isolated single and double bonds are used for reference. To adjust the TRE values to the standard experimental resonance energies of benzene and 1,3,5-triazine and the value attributed to hexazine, scaling factors were introduced[68] for each type of bond.

In this study the R independent force constants used by Bird[68] were replaced for the C–N and N–N bonds with the more realistic values available from Gordon and Ford[27] and Vilkov and Pentin,[70] respectively. As a result of these improvements, the newly derived scaling factors are much closer to each other compared to the values of Bird.[68] The reference data are listed in the Table 8. Both DRE and TRE values are obtained. In TRE calculations, 9.36 kcal mol^{-1} is added to the stabilization energy as recommended by Bird[68] to account for the bond angle strain energy in a five-membered ring. It was expected a priori that DRE should correlate with HOMA, while TRE should be closer to AI, judging by the reference bond lengths. The resonance energies for the azoles are presented in the Table 7 along with the corresponding AI and HOMA values.

The obtained geometric and energetic aromaticity criteria show good linear correlations as illustrated in Fig. 2. The regression characteristics are gathered in the Table 9. A linear relationship is obtained between AI and the 1-GEO term calculated for azoles using the molecular geometries optimized at the SCF/6-31G* level of theory (Fig. 2a). The two outliers correspond to pyrrole and 1*H*-1,2,4-triazole. The former contains three C–C bonds, while the latter is built solely of C–N bonds. Therefore, the deflection is due to the heavily divergent weighting factors attributed to the C–C and C–N bonds in the HOMA calculations.

Similarly, a good linear relationship is observed between AI and 1-GEO calculated with the experimental molecular dimensions (Fig. 2b). No correlation is detected between AI and the EN term. Both AI and (1-GEO) indices consistently indicate that imidazole is less aromatic than pyrrole, 4*H*-1,2,4-triazole is less aromatic than the 1*H*-isomer, etc. Inclusion of the EN term deteriorates the correlation, but not dramatically. It appears reasonable that HOMA and AI give similar relative aromaticities provided that the gas phase molecular geometry is used.

Surprisingly, neither of the two indices correlate with the Dewar resonance energies as obtained within the HOSE model. Instead, both AI and HOMA as well as the 1-GEO term correlate with the TRE values. A plot of the reduced TREs against AIs is given in Fig. 2b. While the AI values are scattered more or less uniformly around the regression

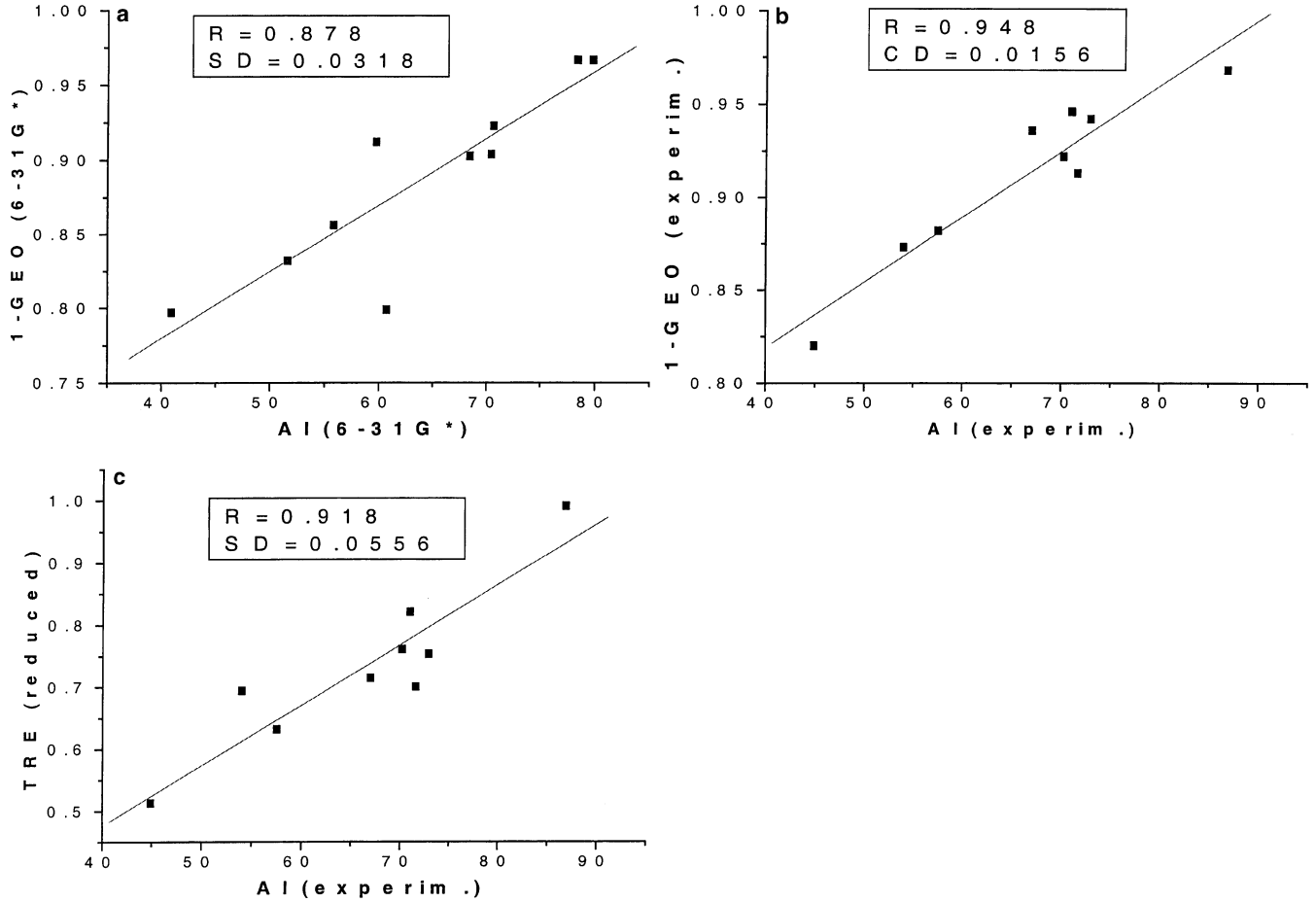

Figure 2. The 1-GEO components of HOMA and Total Resonance Energies for azoles **V**–**XIV** plotted against AI. *R* and CD are the correlation coefficient and standard deviation of the linear regression.

Table 9. Parameters of the linear regression Y=a+bX between the aromaticity indices

Geometry	Y	X	Set	*a*	*b*	*R*	SD
6-31G*	1-GEO	AI	Overall	0.600 (0.056)	4.49×10^{-3} (8.68×10^{-4})	0.878	0.0318
			Except for **I** and **XI**	0.607 (0.018)	4.44×10^{-3} (2.73×10^{-4})	0.989	0.0099
Experim.	1-GEO	AI	Overall	0.678 (0.030)	3.50×10^{-3} (4.47×10^{-4})	0.948	0.0156
	EN	AI	Overall	0.052 (0.040)	-3.77×10^{-4} (5.90×10^{-4})	−0.235	0.0206
	HOMA	AI	Overall	0.627 (0.061)	3.89×10^{-3} (9.07×10^{-4})	0.851	0.0316
	$(TRE)_{Red}$	AI	Overall	0.087 0.107)	9.74×10^{-3} (1.53×10^{-3})	0.918	0.0556
	$(TRE)_{Red}$	1-GEO	Overall	−1.590 (0.448)	2.547 (0.0636)	0.891	0.0636
			Except for **X**	−1.099 (0.310)	1.988 (0.342)	0.922	0.0392
	$(TRE)_{Red}$	HOMA	Overall	−1.056 (0.384)	2.020 (0.433)	0.870	0.0691
			Except for **X**	−0.703 (0.179)	1.597 (0.204)	0.954	0.0302
	$(TRE)_{Red}$	AI	Overall	−0.438 (0.331)	0.016 (0.0049)	0.774	0.1715
	$(TRE)_{Red}$	HOMA	Overall	−2.434 (0.967)	3.446 (1.091)	0.767	0.1740

Values in the brackets denote standard errors.

line, HOMA and its 1-GEO term produce outliers for the highly delocalized 2*H*-1,2,3-triazole. The aromaticity of this molecule is heavily underestimated by HOMA against TRE. The correlation is immediately improved if this molecule is excluded from the set (see Table 9.) Note that neither force constants nor scaling factors presented in the Table 8 provide such divergent contributions for the C–C, C–N and N–N bonds as accepted in HOMA.

The results obtained with HOMA, its GEO term, and TRE support the conclusion deduced above with AI regarding the increase of aromaticity with α aza substitution. For example, the aromaticity systematically decreases in the series 2*H*-1,2,3-triazole>pyrazole≥pyrrole, 1*H*-tetrazole>4*H*-1,2,4-triazole, 2*H*-tetrazole>1*H*-1,2,4-triazole, and so on. On the contrary, β aza substitution in most cases results in clear dearomatization. 4*H*-1,2,4-triazole with two β substitutions is the least aromatic molecule among azoles. Similarly, imidazole is less aromatic than pyrrole, in contrast to the observation of MKWAB.[67] This result is consistent with the ASE values of Katritzky et al.[66] and Pal[71] but contradicts the experimental TRE reported by Bird[68] (the last entry of Table 8). The predicted β aza dearomatization effect in the azole series is opposite to the effect in the azine series reported earlier by Krygowski and Cyranski.[20]

4. Conclusions

The origin of the discrepancies between the Bird and Pozharskii systems of the structural aromaticity indices has been analyzed. Three bottlenecks have been detected, and three simple improvements have been introduced. Two of them are applied to both schemes. The third change is introduced only into the Pozharskii scheme. The modified procedure has been applied to five-membered ring oxygen and nitrogen heterocycles. As a result of the proposed improvements, the discrepancies in AIs are reduced to the difference between the arithmetic and the root-square means of the peripheral bond orders.

Using the refined AIs developed in this work and the currently available molecular geometries, several regularities in the aromaticity of the five-membered heterocycles as a function of both chemical structure and environment have been specified. The aromaticity within the azole series increases in the pyrazole-like structures with adjacent pyrrole- and pyridine-like heteroatoms. The aromaticity decreases for the imidazole-like structure, where the two nitrogens are separated by the carbon atom. In the absence of strong intermolecular hydrogen bonding, peripheral bonds are more localized in the crystal state than in the gas phase. The reverse is true for molecules that are hydrogen bonded in the crystal state. A strong tendency to bond localization in the crystal phase with decreasing temperature is supported by the data.

Ab initio the MP2 molecular geometries better reproduce the mean bond orders of the azole cycles than the SCF geometries. However, the extent of the peripheral bond delocalization is heavily overestimated by MP2. This makes the AIs obtained with the MP2 geometries a good approximation to the aromaticities of the hydrogen-bonded crystal structures rather than to the aromaticities of the free molecules in gas phase.

The generality of the effect of molecular structure on aromaticity has been inspected by comparison with the HOMA indices and resonance stabilization energies. Good correlations have been obtained between the modified AIs and the energetic criteria derived from molecular dimensions.

References

1. Simkin, B. Ya.; Minkin, V. I.; Glukhovtsev, M. N. In *Advances in Heterocyclic Chemistry*; Katritzky, A. R., Ed.; Academic: San Diego, 1993; Vol. 56, pp 303–428.
2. (a) Krygowski, T. M.; Cyranski, M. K. *Chem. Rev.* **2001**, *101*, 1385–1419; (b) Katritzky, A. R.; Jug, K.; Oniciu, D. C. ibid., 1421–1449.
3. Schleyer, P. v. R.; Jiao, H. *Pure Appl. Chem.* **1996**, *68*, 209–218.
4. Lloyd, D. *J. Chem. Inf. Comput. Sci.* **1996**, *36*, 442–447.
5. Krygowski, T. M. *Wiad. Chem.* **1994**, *48*, 719–737.
6. Katritzky, A. R.; Karelson, M.; Malhotra, N. *Heterocycles* **1991**, *32*, 127–161.
7. Gorelik, M. V. *Uspekhi Khimii* **1990**, *59*, 197–228 (in Russian).
8. Jug, K.; Koster, A. M. *J. Phys. Org. Chem.* **1993**, *4*, 163–170.
9. Katritzky, A. R.; Barczynski, P.; Musumarra, G.; Pisano, D.; Szafran, M. *J. Am. Chem. Soc.* **1989**, *111*, 7–15.

10. Galembeck, S. E.; da Costa, Jr., N. B.; Ramos, M. N.; Neto, B. B. *Theochem* **1993**, *101*, 97–104.
11. Caruso, L.; Musumarra, G.; Katritzky, A. R. *Quant. Struct.-Act. Relat.* **1993**, *12*, 146–151.
12. Katritzky, A. R.; Karelson, M.; Wells, A. P. *J. Org. Chem.* **1996**, *61*, 1619–1623.
13. Schleyer, P. v. R.; Freeman, P. K.; Jiao, H.; Goldfuss, B. *Angew. Chem., Int. Ed. Engl.* **1995**, *34*, 337–340.
14. Houk, K. N.; Nendel, M. *Chemtracts: Org. Chem.* **1996**, *9*, 118–120.
15. Bird, S. W. *Tetrahedron* **1996**, *52*, 9945–9952.
16. Krygowski, T. M.; Cieselski, A.; Bird, C. W.; Kotschy, A. *J. Chem. Inf. Comput. Sci.* **1995**, *35*, 203–210.
17. Krygowski, T. M.; Cyranski, M. *Tetrahedron* **1996**, *52*, 1713–1722.
18. Krygowski, T. M.; Cyranski, M.; Wisiorowski, M. *Pol. J. Chem.* **1996**, *9*, 118–120.
19. Krygowski, T. M.; Cyranski, M. *J. Chem. Inf. Comput. Sci.* **1996**, *36*, 1135–1141 see also pp 1142–1145.
20. Krygowski, T. M.; Cyranski, M. *Tetrahedron* **1996**, *52*, 10255–10264.
21. Fringuelli, F.; Marino, G.; Taticchi, A.; Grandolini, G. *J. Chem. Soc., Perkin Trans. 2* **1974**, *2*, 332–337.
22. Pozharskii, A. F. *Khimiya Geterotsikl Soedin.* **1985**, 867–905 (in Russian).
23. Bird, C. W. *Tetrahedron* **1985**, *41*, 1409–1414.
24. Bird, C. W. *Tetrahedron* **1992**, *48*, 335–340.
25. Ostrovskii, V. A.; Yerusalimskii, G. B.; Scherbinin, M. B. *Zhurn. Organicheskoi Khimii* **1995**, *31*, 1422–1431 (in Russian).
26. Gordy, W. *J. Chem. Phys.* **1947**, *15*, 305–310.
27. Gordon, A. J.; Ford, R. A. *The Chemist's Companion. A Handbook of Practical Data, Techniques, and References*; Wiley: New York, 1972.
28. Kitaygorodskii, A. I.; Zorkii, P. M.; Belskii, V. K. *The Structure of Organic Substance. Structural Data of 1929–1970*; Nauka: Moscow, 1980 (in Russian). Kitaygorodskii, A. I.; Zorkii, P. M.; Belskii, V. K. *Structural Data of 1971–1973*; Nauka: Moscow, 1982 (in Russian).
29. Vilkov, L. V.; Mastryukov, V. S.; Sadova, N. I. *Determination of the Geometry of Free Molecules*; Khimiya: Leningrad, 1978 (in Russian).
30. Allen, F. H.; Kennard, O.; Watson, D. G.; Brammer, L.; Orpen, G.; Taylor, R. *J. Chem. Soc., Perkin Trans. 2* **1987**, S1–S19.
31. March, J. *Advanced Organic Chemistry: Reactions, Mechanisms and Structure*; 3rd ed; Wiley: New York, 1985.
32. Microcal™ ORIGIN™ Version 5.0, Copyright 1991–1997, Microcal Software Inc.
33. Box, V. G. S. *Heterocycles* **1991**, *32*, 2023–2041.
34. Witanowski, M.; Biedrzycka, Z. *Magn. Reson. Chem.* **1994**, *32*, 62–66.
35. Liebling, G.; Marsh, R. E. *Acta Crystallogr.* **1965**, *19*, 202–205.
36. Krygowski, T. M.; Cyranski, M. K. *Tetrahedron* **1999**, *55*, 11143–11148.
37. Mo, O.; dePaz, J. L. G.; Yanez, M. *J. Phys. Chem.* **1986**, *90*, 5597–5604.
38. Bean, J. P. *J. Org. Chem.* **1998**, *63*, 2497–2506.
39. Lipkowitz, K. B.; Naylor, A. M.; Melchior, W. B. *Tetrahedron Lett.* **1984**, *25*, 2297–2300.
40. Fourme, P. R. *Acta Crystallogr.* **1972**, *B28*, 202–205.
41. Chrisren, D.; Griffits, J.; Sheridan, J. *Z. Naturforsch.* **1982**, *37A*, 1378–1385.
42. Popik, N. I.; Shablygin, M. V.; Vilkov, L. V.; Semenova, A. S.; Kravchenko, T. V. *Vysokomol. Soedin.* **1983**, *B52*, 38–40 (in Russian).
43. Batsanov, A. S.; Struchkov, Yu. T.; Gakh, A. A.; Fainzilberg, A. A. *Izv. Russ. Akad. Nauk, Ser. Khim.* **1994**, 639–641.
44. Nagy, P. I.; Durant, G. J.; Smith, D. A. *J. Am. Chem. Soc.* **1993**, *115*, 2912–2922.
45. Nygaard, L.; Christen, D.; Nielsen, J. T.; Pedersen, E. J.; Snerling, O.; Vestergaard, E.; Sørensen, G. O. *J. Mol. Struct.* **1974**, *22*, 401–413.
46. Larsen, F. K.; Lehmann, M. S.; Sotofte, I.; Rasmussen, S. E. *Acta Chem. Scand.* **1970**, *24*, 3248–3258.
47. El-Bakali Kassimi, N.; Doerksen, R. J.; Thakkar, A. J. *J. Phys. Chem.* **1995**, *99*, 12790–12796.
48. Will, G. *Z. Kristallographie* **1969**, *129*, 211–221.
49. Martinez-Carrera, S. *Acta Crystallogr.* **1966**, *20*, 783–789.
50. McMullan, R. K.; Epstein, J.; Ruble, R.; Craven, B. M. *Acta Crystallogr. B* **1979**, *35*, 688–691.
51. Begtrup, M.; Nielsen, C. J.; Nygaard, L.; Samdal, S.; Sjøgren, C. E.; Sørensen, G. O. *Acta Chem. Scand.* **1988**, *42A*, 500–514.
52. Törnkvist, C.; Bergman, J.; Liedberg, B. *J. Phys. Chem.* **1991**, *95*, 3123–3128.
53. Albert, A.; Taylor, P. J. *J. Chem. Soc., Perkin Trans. 2* **1989**, 1903–1905.
54. Bolton, K.; Brown, R. D.; Burden, F. R.; Mishra, A. *J. Chem. Soc. Chem. Commun.* **1971**, 873. Bolton, K.; Brown, R. D.; Burden, F. R.; Mishra, A. *J. Mol. Struct.* **1975**, *27*, 261–266.
55. Deuschl, H. *Ber. Bunsenges. Physik. Chem.* **1965**, *69*, 550–557.
56. Goldstein, P.; Ladell, J.; Abovitz, G. *Acta Crystallogr. B* **1966**, *25*, 135–143.
57. Ponomaryov, O. A.; Borovkov, A. V.; Doroshenko, A. O.; Baumer, V. N.; Mitina, V. G.; Surov, Yu. N.; Pivnenko, N. S. *Mol. Engng* **1994**, *3*, 343–352.
58. Wong, M. W.; Leung-Toung, R.; Wentrup, C. *J. Am. Chem. Soc.* **1993**, *115*, 2465–2472.
59. Tornkvist, C.; Bergman, J.; Liedberg, B. *J. Phys. Chem.* **1991**, *95*, 3119–3123.
60. *Comprehensive Organic Chemistry: The Synthesis and Reaction of Organic Compounds*; Barton, D., Ollis, W. D., Eds.; Heterocyclic Compounds, Pergamon: Oxford, 1979; Vol. 4.
61. Krygowski, T. M. *J. Chem. Inf. Comput. Sci.* **1993**, *33*, 70–78.
62. Epiotis, N. D.; Cherry, W. R.; Bernardi, F.; Hehre, W. J. *J. Am. Chem. Soc.* **1976**, *98*, 4361–4364.
63. Nyulashi, L.; Varnai, P.; Veszpremi, T. *Theochem* **1995**, *358*, 55–61.
64. Griffiths, J. *Dyes and Pigments* **1982**, *3*, 211–233.
65. Ferris, K. F.; Bartlett, R. J. *J. Am. Chem. Soc.* **1992**, *114*, 8302–8303.
66. Katritzky, A. R.; Karelson, A. R.; Sild, S.; Krygowski, T. M.; Jug, K. *J. Org. Chem.* **1998**, *63*, 5228–5231.
67. Mrozek, A.; Karolak-Woiciechowska, J.; Amiel, P.; Barbe, J. *J. Mol. Struct.* **2000**, *524*, 151–157.
68. Bird, C. W. *Tetrahedron* **1997**, *53*, 13111–13117.
69. Krygowski, T. M.; Wieckowski, T. *Croat. Chim. Acta* **1981**, *54*, 193–202.
70. Vilkov, L. V.; Pentin, Yu. A. *Instrumental Technique of Chemistry: The Structural Methods and Optical Spectroscopy*; Visshaya Shkola: Moscow, 1987 (in Russian).
71. Pal, S. K. *Theochem.* **1998**, *434*, 85–93.